Duration and Magnitude of Myofascial Release in 3-Dimensional Bioengineered Tendons: Effects on Wound Healing

Thanh V. Cao, BSc; Michael R. Hicks, PhD; Manal Zein-Hammoud, PhD; and Paul R. Standley, PhD

From the Department of Basic Medical Sciences at the University of Arizona College of Medicine in Phoenix (Mr Cao and Drs Zein-Hammoud and Standley) and the Department of Molecular and Cell Biology at Arizona State University in Tempe (Dr Hicks).

Financial Disclosures: None reported.

Support: Funding for this study was provided by the American Osteopathic Association (grant 1121640).

Address correspondence to Paul R. Standley, PhD, Department of Basic Medical Sciences, Univeristy of Arizona College of Medicine, B-558 HSEB, 435 N 5th St, Phoenix, AZ 85004-2157.

E-mail: standley@email.arizona.edu

Submitted August 28, 2013; final revision received October 10, 2014; accepted November 14, 2014.

Context: Myofascial release (MFR) is one of the most commonly used manual manipulative treatments for patients with soft tissue injury. However, a paucity of basic science evidence has been published to support any particular mechanism that may contribute to reported clinical efficacies of MFR.

Objective: To investigate the effects of duration and magnitude of MFR strain on wound healing in bioengineered tendons (BETs) in vitro.

Methods: The BETs were cultured on a deformable matrix and then wounded with a steel cutting tip. Using vacuum pressure, they were then strained with a modeled MFR paradigm. The duration of MFR dose consisted of a slow-loading strain that stretched the BETs 6% beyond their resting length, held them for 0, 1, 2, 3, 4, or 5 minutes, and then slowly released them back to baseline. To assess the effects of MFR magnitude, the BETs were stretched to 0%, 3%, 6%, 9%, or 12% beyond resting length, held for 90 seconds, and then released back to baseline. Repeated measures of BET width and the wound's area, shape, and major and minor axes were quantified using microscopy over a 48-hour period.

Results: An 11% and 12% reduction in BET width were observed in groups with a 9% (0.961 mm; $P<.01$) and 12% (0.952 mm; $P<.05$) strain, respectively. Reduction of the minor axis of the wound was unrelated to changes in BET width. In the 3% strain group, a statistically significant decrease (–40%; $P<.05$) in wound size was observed at 24 hours compared with 48 hours in the nonstrain, 6% strain, and 9% strain groups. Longer duration of MFR resulted in rapid decreases in wound size, which were observed as early as 3 hours after strain.

Conclusion: Wound healing is highly dependent on the duration and magnitude of MFR strain, with a lower magnitude and longer duration leading to the most improvement. The rapid change in wound area observed 3 hours after strain suggests that this phenomenon is likely a result of the modification of the existing matrix protein architecture. These data suggest that MFR's effect on the extracellular matrix can potentially promote wound healing.

J Am Osteopath Assoc. 2015;115(2):72-82
doi:10.7556/jaoa.2015.018

Myofascial release (MFR) is a common technique in manual medicine used to treat patients with various soft tissue disorders. The technique involves slowly applying an external mechanical load that overcomes the fascia or tendon's intrinsic tension to lengthen the collagen fibers.[1] Myofascial release is designed to actively stretch and elongate the fascia and underlying soft tissue to release areas of decreased fascial motion. Documented clinical outcomes associated with MFR include improved physiologic function, reduction of pain, and increased range of motion in the affected joint.[2,3] To our knowledge, clinical findings that directly implicate MFR in enhanced wound healing have not been documented. However, clinical studies using vacuum compression therapy, which uses similar mechanical stretch parameters, suggests a potential correlation between biomechanical strain and enhanced wound healing.[4-7]

Fibroblasts play an important role in wound healing and in the regulation of the local inflammatory response.[8,9] As the primary cell type in connective tissue, fibroblasts maintain and restore the tissue's structural homeostasis through the synthesis, degradation, and reorganization of the extracellular matrix.[10] In addition, the ability of fibroblasts to respond to mechanical stimuli by modifying gene expression[11-13] makes them likely targets for the mechanotransduction of MFR. In previous studies[12,13] we used 2-dimensional fibroblast tissue constructs to identify the mechanisms behind the clinical efficacy of MFR. Our previous findings revealed that modeled MFR applied in vitro inhibits the cytotoxic effects of fibroblasts, alters fibroblast actin architecture, and induces the expression of various anti-inflammatory and growth factors.[12,13] We have also shown that MFR downregulates inhibitory factors on protein kinase C and phosphoinositide 3-kinase to sensitize fibroblasts to nitric oxide and improve wound healing.[14] These findings highlight mechanisms that may support the clinical effectiveness of MFR.

In vivo, fibroblasts exist in a 3-dimensional extracellular matrix, which serves as a vital biomechanical feedback system that dictates signaling and adaptive response in wound repair.[15] In our previous studies[12,15] we used 2-dimensional fibroblast tissue constructs on which a modeled MFR of a single strain magnitude and duration setting was applied. Various rates of manual manipulative treatment can induce different degrees of sympathetic efferent nerve stimulation and blood flow.[16] Recent data from our laboratory have also shown that in a 3-dimensional environment, fibroblast cytokine secretion is dependent on MFR strain duration and magnitude,[17] suggesting a correlation between physiologic response and dosed MFR. Results from our 2-dimensional studies[14] provide evidence to support improved wound-healing rates using a single MFR treatment; however, the cellular mechanisms that link MFR to wound closure were not identified, owing to the single strain parameter tested and the lack of dimensionality.

In the present study, we improved on our strain model and in vitro tissue system by investigating the effects of MFR strain duration and magnitude using a 3-dimensional bioengineered tendon (BET) wound model. We hypothesized that a unique MFR strain regimen would result in unique wound-healing responses. We expected the results of this study to help elucidate the potential efficacy of MFR on muscle fascia and tendon wound repair.

Methods

The current study was conducted between October 2010 and January 2013.

Cell Culture and Fabrication of BETs

All experiments were conducted using commercially available normal human dermal fibroblasts. Cells were cultured at 37°C, 5% CO_2, and 100% humidity in Dulbecco's modified Eagle's medium supple-

mented with 2% fetal bovine serum and 1% penicillin-streptomycin. The medium was replaced with fresh prewarmed growth medium every 2 days. Confluent cultures (acquired within 7-10 days) were passaged at a ratio of 1:3, and all experiments used cell passages between 4 and 10.

Normal human fibroblasts at a concentration of 1000 cells/μL were mixed in a solution of 70% Purecol collagen type I (Advanced Biomatrix, Inc) and 30% 5× Dulbecco's modified Eagle's medium to create a collagen-fibroblast gel. A loading channel was created for the gel using a linear Trough Loader (Flexcell International Corp) placed beneath the Tissue Train Plates (Flexcell International Corp). These 6-well formatted plates consisted of flexible elastomeric well bottoms that were attached to nondeformable nylon mesh anchors at each end of the long axis. To create a cylindrical structure attached at the 2 anchors, 200 μL of the collagen-fibroblast gel were then added to the loading channel and allowed to polymerize for 2 hours in a humidified 37°C incubator. After the gel matrix polymerized, the vacuum was released, thereby allowing the BETs to be free from all attachments except at the 2 anchor points. Fresh culture medium supplemented with 2% fetal bovine serum was then added to each well, and the BETs were allowed to acclimate for 24 to 48 hours before undergoing MFR.

To study the effect of fibroblasts in remodeling of the overall structure of BETs, we developed fibroblast-free BETs made entirely of Purecol collagen. These fibroblast-free BETs revealed the difference in structure of BETs in the presence and absence of fibroblasts (*Figure 1A*).

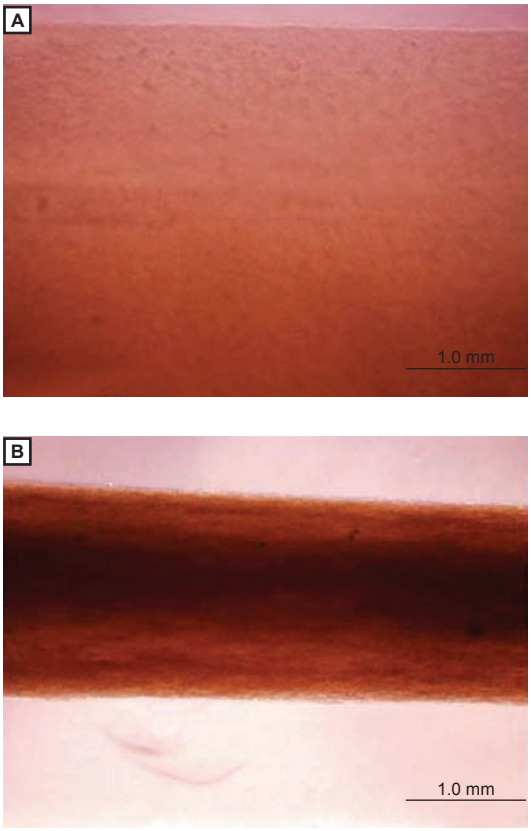

Figure 1.
Photomicrographs of (A) fibroblast-free bioengineered tendon (BET) and (B) fibroblast-containing BET after 48 hours of acclimation (original magnification ×40). Note the equality of scale bars.

BET Wounding Protocol

An artificial wound was created using a sterile stainless steel cutting tip. The apparatus had a circular cutting diameter of 0.75 mm and a cutting area of 0.442 mm^2. A soft self-healing cutting mat was placed directly under the tissue and held steadily with sterile forceps. The cutting tip was positioned perpendicularly to the BET and slowly pressed onto the tissue in a gentle rotating motion until the cutting tip penetrated the BET and made contact with the underlying cutting mat. The cutter was then slowly lifted away from the BET to create an area completely devoid of fibroblasts and extracellular matrix at the approximate center of the BET (*Figure 2A*). Photomicrographs were captured immediately after wounding to establish a baseline wound size for each BET. The BETs were then assigned to 1 of the following groups: strain duration, strain magnitude, or nonstrain.

Study Groups

For the strain duration groups, strain was slowly applied to elongate the tissue to 2.5% of its resting length per second to reach a maximum 6% strain (ie, to 106% of its initial resting length). The BET was then held at 6% elongation for 1, 2, 3, 4, or 5 minutes. The strain was then slowly released back to baseline at a rate of –1.5% per second. For the strain magnitude groups, a slow-loading strain was similarly applied until a maximum magnitude of 3%, 6%, 9%, or 12% elongation was reached. The maximum strain was held for 90 seconds and then allowed to slowly release back to baseline using the identical unloading rate noted above. The nonstrained BETs served as controls.

Biomechanical Strain Paradigm

The baseline algorithm of the in vitro MFR paradigm was determined by quantitative analysis of videomorphic recordings of clinically applied MFR.[12] From these findings, we defined the strain frequency, direction, and loading rates of the modeled MFR and applied them in vitro using the Flexercell FX-4000 Tension Plus System (Flexcell International Corp). The BETs were stretched uniaxially in the direction of their long axis by placing a loading post beneath the elastomeric well bottom and applying negative pressure. The pressure increased the distances between the 2 opposite nondeformable anchors to which the BET was attached.

Analysis of Wound Area and Dimensions

The average tissue width of the entire BET was measured at the center of the wound and at approximately 2 mm to the right and left of the center location using ImageJ (National Institutes of Health). To assess wound closure over time, photomicrographs were captured using an IX71 Olympus inverted microscope and DP71 camera (Olympus America Inc) immediately after injury (T0) and again at 3 (T3), 18 (T18), 24 (T24), and 48 (T48) hours after MFR (*Figure 2A* and *Figure 2B*). Images were then converted to black and white with Adobe Photoshop CS2 ver-

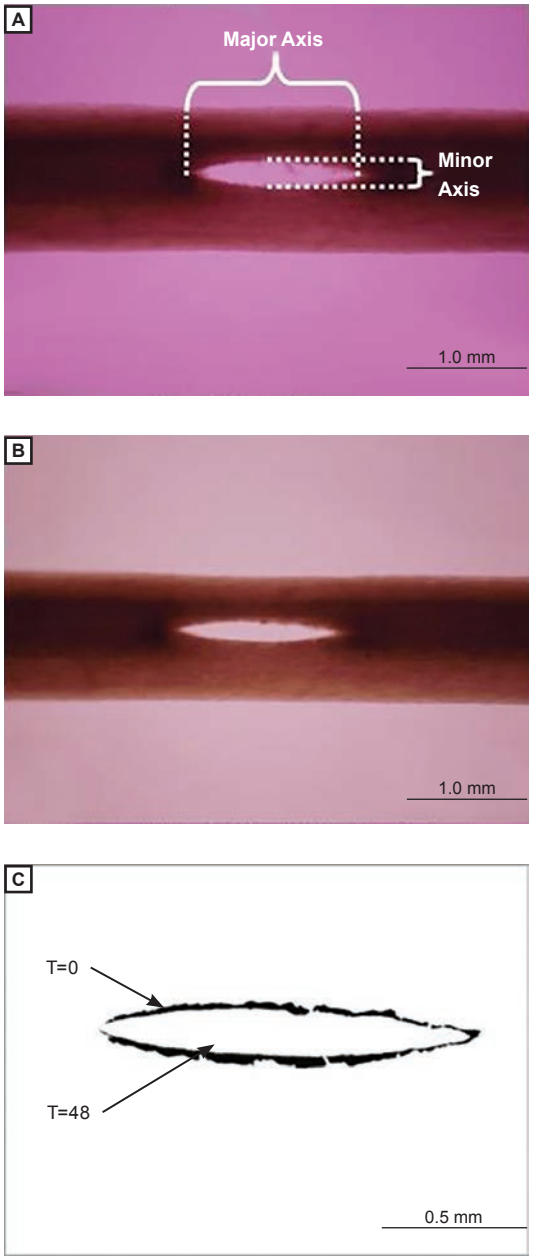

Figure 2.
(A) Nonstrained bioengineered tendon (BET) immediately after wounding. White brackets indicate the direction of the wound's major and minor axes. (B) Nonstrain BET 48 hours after wounding. (C) Wound outlines at time 0 and 48 hours were determined via CellProfiler (Broad Institute Imaging Platform) and overlaid. The black shaded area represents the decrease from the original wound size during this period. Forty-eight hours after treatment, the major axis of the wound was 1.31 mm; minor axis of the wound, 0.163 mm; wound size, 0.148 mm^2; percent decrease from original size, 28.8; and smoothing filter size, 1.3.

sion 9.0 (Adobe Systems Inc) and analyzed for wound closure using CellProfiler analysis software (Broad Institute Imaging Platform) (*Figure 2C*). The CellProfiler algorithm detected the BET wound edges based on pixel tone and color, enabling the measurement of the overall wound area. The CellProfiler also quantified the length of the long (major) and short (minor) axes of the elliptical wound. In addition, the area eccentricity ratio (AER; how much the area deviates from its original shape) of the elliptical wound was determined by dividing the actual wound area by the theoretical area of a true ellipse as determined according to the major and minor axes as follows: area = ½(major axis) ½(minor axis) π.

An AER greater or less than 1 signified that the wound shape deviated from its original elliptical shape, where AER values greater than 1 were more linear and AER values less than 1 were more circular.

Statistical Analysis

Data were compared by a *t* test and 1-way analysis of variance using post hoc Dunnett tests (Prism 4.03, GraphPad Software, Inc). Group means with $P<.05$ determined by analysis of variance were verified by *t* tests and were considered to be statistically significant.

Results

Data are given as mean [SD] unless otherwise indicated.

Presence of Fibroblasts

The overall structure of BETs was remodeled in the presence of fibroblasts. The wounds took on an elliptical shape immediately after wounding (*Figure 2A*). In the nonstrain BETs, an approximate 30% decrease in wound size was observed during a 48-hour period (*Figure 2B* and *Figure 2C*). The collagen gel constructs grown in the presence of fibroblasts and allowed to acclimate for 48 hours showed a gradual reduction in overall tissue width over time. There was an approximate 72% reduction in tendon width (data not shown), with the structure appearing less transparent than the fibroblast-free BETs (*Figure 1A*). In addition, the fibroblast-free BETs appeared less defined and more gelatinous in structure compared with fibroblast-containing BETs (*Figure 1B*). Fibroblast-containing BETs appeared to show greater stiffness than fibroblast-free BETs, and once the tissue was detached from its anchor points, it immediately shifted to an arch shape, suggesting that inherent tension develops only in fibroblast-containing BETs (data not shown).

Strain

Large-Magnitude Strain Reduced BET Thickness In Vitro

Immediately after MFR, the BETs took on a hairpinlike appearance, forming a bulge at the wound site. However, owing to the elastic nature of the construct, the tissue slowly recoiled back to its original length. Forty-eight hours after MFR, there were no observed differences in BET width among any of the strain duration groups and the nonstrain group. In the 3% and 6% strain magnitude groups, there were no observed differences in BET width compared with the nonstrain group. However, we observed an 11% (0.961 [0.024] mm; $P<.01$) and 12% (0.952 [0.048] mm; $P<.05$) reduction in the average BET width at the center of the wound in the 9% and 12% strain magnitude groups, respectively, compared with the nonstrain (1.08 [0.035] mm), 3% (1.09 [0.040] mm), and 6% strain magnitude (1.08 [0.030] mm) groups (*Figure 3* and *eTable 1*).

Low-Magnitude and Long-Duration Strain Hastened Wound Closure

In the strain magnitude groups, it was observed that in the 12% group, the major axis of the wound increased immediately after the cessation of MFR and gradually continued to increase for 18 hours. At this peak, the major axis was approximately 44.2% (T0=1.13 [0.106] mm vs T24=1.59 [0.067] mm; $P<.05$) longer than that of the original wound. No changes to the major axis of

the wound were observed in the nonstrain or in any of the other strain magnitude groups. A statistically significant decrease in the minor axis of the wound was consistent with lower-magnitude strain. At 3% and 6% magnitude, a statistically significant decrease in the minor axis was seen as early as 18 hours compared with the original wound size. When the strain was increased to 9%, changes in the minor axis were not observed until 24 hours after cessation of the strain, and at 12%, no changes were observed at any time point (*Table 1*). When strain magnitude was held constant, increasing the duration of MFR strain did not statistically significantly alter the length of the major axis of the wound in any of the groups. All groups displayed a gradual decrease in the minor axis over time; however, the earliest statistically significant decrease was found to occur at 24 hours in the 5-minute MFR group (33%, 0.10 [0.014] mm vs 0.15 [0.010] mm; $P<.05$; *Table 2*). All other groups resulted in a reduction of the minor axis, ranging from 33% to 43% ($P<.05$) 48 hours after MFR.

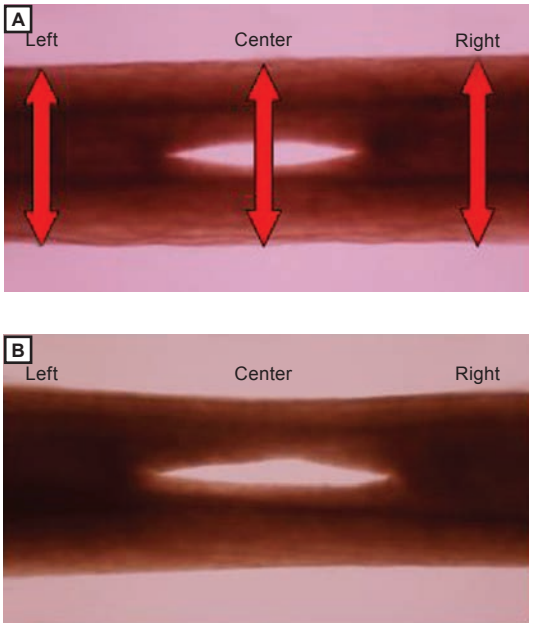

Figure 3.
Bioengineered tendon (BET) 48 hours after wounding (nonstrain [A] and 12% strain [B]). Width measurements were obtained at the center of the wound and at the left and right margins of the wound as indicated by the red arrows in image A.

Large-Magnitude Strain Slowed BET Wound Closure Rates

Wound closure rate was determined by comparing the wound sizes of each group with the nonstrain group at each corresponding time point (3, 18, 24, or 48 hours). Wound closure rate was also determined by identifying the earliest time point at which a statistically significant decrease or increase in wound size was observed compared with the initial wound size. Myofascial release designed to stretch BETs 3% to 9% beyond their initial resting length for 90 seconds displayed no differences in wound closure compared with nonstrain. However, in the 12% group, the wound size was significantly larger than the nonstrain group at all time points measured ($P<.05$). Comparing the wound sizes at various duration intervals after MFR with the original wound size, the 3% magnitude group showed a statistically significant reduction in the initial wound size by 24 hours (–43.46% [23.6]; $P<.05$). Nonstrain, 6%, and 9% magnitude groups showed a statistically significant decrease in wound size by 48 hours. The 12% strain group showed a 29.5% (46.89) increase in wound size 3 hours after strain compared with the original wound (*Figure 4* and *eTable 2*).

Long-Duration Strain Resulted in Rapid Changes in Wound Area and Shape

When keeping the magnitude constant at 6% elongation, a 1-minute strain resulted in a statistically significant reduction in wound size 48 hours after MFR (–51.9% [24.79]; $P<.05$). Increasing strain duration to 3 minutes resulted in –42.1% [20.15]; $P<.05$) wound closure at 18 hours after MFR. The 5-minute strain resulted in a rapid reduction in wound size (–40.1% [17.8]; $P<.05$) that was observed 3 hours after MFR. The 1-minute strain was no more effective than the nonstrain.

Table 1.
Measurements of the Wound Axes in Bioengineered Tendons Undergoing Myofascial Release by Strain Magnitude at 90 s Duration

	Wound Measurement (Mean [SEM] mm) by Follow-Up				
Magnitude	**0 h**	**3 h**	**18 h**	**24 h**	**48 h**
Major Axis					
Nonstrain	1.18 (0.052)	1.17 (0.067)	1.12 (0.076)	1.11 (0.082)	1.13 (0.070)
3%	1.35 (0.103)	1.25 (0.118)	1.14 (0.148)	1.18 (0.132)	1.19 (0.129)
6%	1.18 (0.037)	1.23 (0.077)	1.18 (0.105)	1.17 (0.112)	1.12 (0.114)
9%	1.33 (0.047)	1.38 (0.106)	1.44 (0.102)	1.42 (0.103)	1.38 (0.097)
12%	1.13 (0.106)	1.37 (0.088)	1.59 (0.067)[a]	1.63 (0.071)[a]	1.57 (0.067)[a]
Minor Axis					
Nonstrain	0.19 (0.011)	0.19 (0.014)	0.16 (0.014)	0.16 (0.014)	0.14 (0.014)[b]
3%	0.25 (0.020)	0.21 (0.025)	0.17 (0.027)[b]	0.16 (0.024)[b]	0.14 (0.021)[b]
6%	0.21 (0.014)	0.18 (0.014)	0.15 (0.015)[b]	0.14 (0.016)[b]	0.12 (0.087)[b]
9%	0.23 (0.018)	0.18 (0.021)	0.16 (0.119)	0.15 (0.179)[b]	0.13 (0.015)[b]
12%	0.23 (0.015)	0.21 (0.016)	0.20 (0.17)	0.20 (0.016)	0.19 (0.016)

[a] Significant increase (P<.05) compared with the pretreatment wound axes at time 0.
[b] Significant decrease (P<.05) compared with the pretreatment wound axes at time 0.

However, in the 3-, 4-, and 5-minute groups, we observed that the percent decrease in wound area was more prominent than that in the nonstrain group when compared as early as 3 hours after MFR (*Figure 5* and *eTable 3*). Comparing the AER revealed no changes with magnitude dosing from before MFR to 3 hours after MFR (*Figure 6*). However, in the strain duration groups, we observed a decreasing AER trend in MFR applications that were longer than 2 minutes (*Figure 7*).

Discussion

The current study investigated the influences of MFR strain duration and magnitude on BET wound healing in vitro and found that lower-magnitude and longer-duration MFR strain is associated with accelerated wound closure rates. Longer-duration MFR caused a rapid change in wound morphology as shown by decreased overall wound size measured at 3 hours after MFR. In contrast, larger-magnitude MFR exacerbated the original wound by further enlarging the site of injury.

The ability of fibroblasts to respond to mechanical stimuli and their involvement in wound repair, inflammation, and matrix contraction[12,13] identify them as likely targets for mechanistic studies in manual medicine. Our laboratory has been studying the response of fibroblasts to mechanical stimuli, particularly MFR in both 2- and 3-dimensional matrices.[14,17] In the present study, we used a 3-dimensional tissue construct to more closely mimic a physiologically relevant system. The 3-dimensional extracellular matrix found in vivo provides an important environment for biome-

Table 2.
Measurements of the Wound Axes in Bioengineered Tendons Undergoing Myofascial Release by Strain Duration at 6% Magnitude

	Wound Measurement (Mean [SEM] mm) by Follow-Up				
Duration	**0 h**	**3 h**	**18 h**	**24 h**	**48 h**
Major Axis					
Nonstrain	1.18 (0.052)	1.17 (0.067)	1.12 (0.076)	1.11 (0.082)	1.13 (0.070)
1 min	1.09 (0.120)	1.09 (0.120)	1.11 (0.109)	1.09 (0.118)	1.21 (0.130)
2 min	1.04 (0.126)	1.02 (0.131)	0.99 (0.138)	0.96 (0.132)	0.91 (0.160)
3 min	0.95 (0.116)	0.91 (0.119)	0.88 (0.548)	0.86 (0.535)	0.91 (0.131)
4 min	0.97 (0.123)	0.98 (0.113)	1.02 (0.118)	1.04 (0.139)	0.97 (0.134)
5 min	0.97 (0.056)	0.91 (0.079)	0.96 (0.077)	0.87 (0.093)	0.77 (0.120)
Minor Axis					
Nonstrain	0.19 (0.011)	0.19 (0.014)	0.16 (0.014)	0.16 (0.014)	0.14 (0.014)[a]
1 min	0.21 (0.018)	0.21 (0.018)	0.17 (0.017)	0.16 (0.018)	0.14 (0.021)[a]
2 min	0.19 (0.024)	0.18 (0.027)	0.15 (0.022)	0.13 (0.022)	0.11 (0.021)[a]
3 min	0.17 (0.019)	0.15 (0.024)	0.13 (0.024)	0.12 (0.023)	0.11 (0.019)[a]
4 min	0.16 (0.024)	0.15 (0.027)	0.13 (0.021)	0.13 (0.024)	0.09 (0.046)[a]
5 min	0.15 (0.010)	0.13 (0.016)	0.11 (0.015)	0.10 (0.014)[a]	0.08 (0.011)[a]

[a] Significant decrease ($P<.05$) compared with pretreatment wound axis at time 0.

chanical feedback mechanisms in regulating fibroblast proliferation, migration, differentiation, and signaling responses.[18-20] The matrix also affects the diffusion of regulatory soluble mediators through ligand binding within the matrix that can alter the local concentration gradient of inflammatory cytokine and growth factors secreted by fibroblasts.[21,22] Immediately after excising the BETs with a circular cutting apparatus, the resulting wound took on an elliptical shape and had a smaller area than the cutting apparatus. Bush et al[23] found that the natural line of tension in skin, also known as a Langer line,[24,25] causes wounds to collapse when the extracellular matrix is disrupted, resulting in a smaller elliptical wound. The wound in our model behaved similarly to skin tissue, suggesting that fibroblasts may have been contracting or remodeling the extracellular matrix to generate tension in the BETs (*Figure 1B*). This phenomenon was not present in fibroblast-free BETs (*Figure 1A*), suggesting that fibroblasts are required for active remodeling of the extracellular matrix.

Myofascial release altered the wound closure rate in dose-dependent manners. In the strain magnitude group, faster wound closure time correlated with lower strain magnitudes (3% and 6%) and reduction in the minor axis of the wound (*Table 1*). This phenomenon was unrelated to the changes in the width of the overall structure of the BET as observed with the 12% magnitude group, which showed narrowing of the BET, exacerbating of the wound size, and lengthening of the major axis of

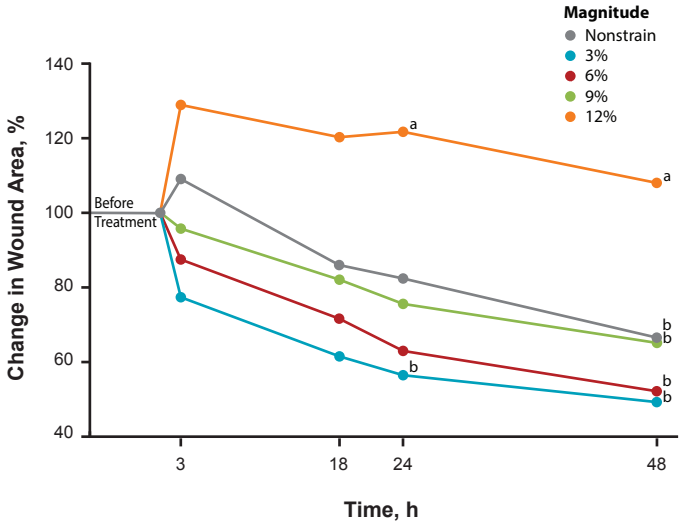

Figure 4.
Wounded bioengineered tendons treated with 0% (nonstrain), 3%, 6%, 9%, or 12% myofascial release for 90 seconds. Change in wound area measured as a percent change from time 0 (100%) measured 3, 18, 24, and 48 hours after myofascial release. Data are given as mean (SD). [a]Statistically significant increase ($P \leq .03$) in wound area compared with time 0. [b]Statistically significant decrease ($P < .05$) in wound area compared with time 0.

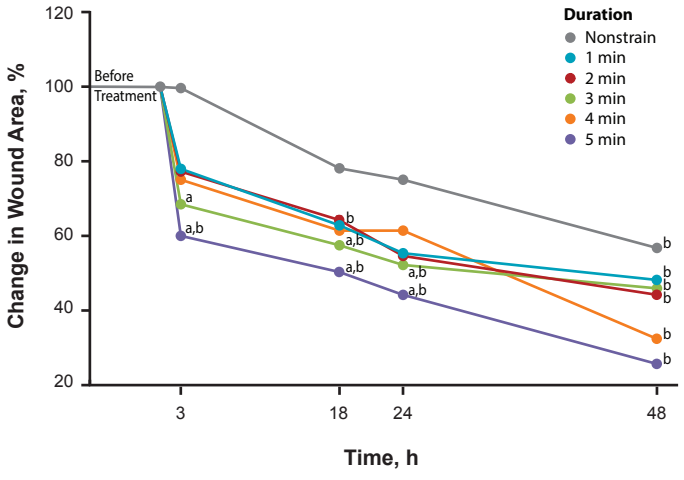

Figure 5.
Wounded bioengineered tendons treated with nonstrain, 1, 2, 3, 4, or 5 minutes of myofascial release stretch 6% beyond its initial resting length. Changes in wound area measured as a percent change from time 0 (100%) measured 3, 18, 24 and 48 hours after myofascial release. [a]Statistically significant decrease ($P \leq .03$) in wound area compared with time 0. [b]Statistically significant decrease ($P \leq .05$) in wound area compared with time 0.

the wound (*Figure 3* and *Table 1*). Smith et al[26] found that extraneous mechanical strain can lead to disassembly of larger-diameter fibrils. In addition, a strain magnitude greater than 10% causes thinning of collagen fibril diameter, whereas 0% to 5% strain has no effect.[27] This finding offers a possible explanation as to why we observed a narrowing of the BET width in the 12% magnitude group, whereas a magnitude of 3% to 9% resulted in no measurable changes.

We found that a longer duration of MFR resulted in rapid changes in the shape and measurable wound area (*Figure 4*, *Figure 6*, *Figure 7*, and *eTable 2*). These rapid responses to architectural change suggest that this phenomenon cannot be attributed to gene activation or modification, owing to the short time that had elapsed since MFR. However, the possibility of MFR activating an ectocytotic process to secrete membrane-bound matrix vesicles or to modify existing matrix protein architecture cannot be ruled out. This process has been shown to occur as rapidly as 5 minutes after stress-relaxation.[28] The release of matrix vesicles is typically observed when fibroblasts differentiate into the contractile phenotype (myofibroblast) to induce extracellular matrix remodeling. It is possible that MFR held for longer than 2 minutes may simulate the mechanical stress signals that are generated by myofibroblasts to trigger early matrix remodeling. Another potential explanation could be the ability of mechanical strain to decrease cell/extracellular matrix attachment. In vivo, fibroblasts bind to multiple collagen filaments that cross-link numerous fibers to dictate the tissues' resting texture, tension, and shape. Mechanical tension is known to affect cell orientation and to decrease cytoskeleton rigidity and viscosity and extracellular matrix contact points.[11-13,29] The reduction in fibroblast contact with the extracellular matrix and the decrease in cell shape stability could cause the wound to collapse, resulting in a change in wound shape. Studies investigating focal adhesion kinase and integrin interaction with the extracellular matrix are in progress in our laboratory. We are also interested in histologic analysis to quantify the reorganization of the preexisting extracellular matrix protein as well as to quantify the newly synthesized collagen.

The limitations of using in vitro models to correlate with in vivo wound-healing responses include the lack of blood and tissue fluid dynamics as well as the lack of other cell types (eg, neutrophils, macrophages, epithelial cells) that significantly contribute to chemotaxis, inflammation, and wound healing. Age, physique, and countless other patient variables also play important roles in manual treatments because each patient's body type possesses distinct fascial and muscle tone and density. These physical variations may also affect how the soft tissue opposes the biomechanical maneuver applied by the physician. These factors were beyond the scope of this study. This model allowed us to negate the effects of age, tissue integrity, and external environmental factors to allow the application of a reproducible MFR protocol and to focus on the direct effects of strain on fibroblast-mediated wound healing.

Conclusion

The results of the current study provide evidence to suggest that different parameters of MFR induce unique wound-healing responses and an optimal MFR strain magnitude and duration exists that results in optimal wound healing. The BET wound-healing rates were hastened when a lower magnitude and longer duration of MFR strain were applied. Larger magnitudes of MFR strain resulted in enlarging the wound size and exacerbating the site of injury. If the results of the current study are clinically translatable, they suggest that MFR significantly affects tendon wound healing in manners that are dependent on both duration and magnitude. These data provide preliminary evidence to suggest that there may be an optimal biomechanical range at which MFR yields the maximum beneficial outcomes, thus supporting a need for individualized MFR. Clinical studies have been vital in establishing the efficacy of manual manipulative treatments; however, such studies have not yet looked at variables such as magnitude and duration of MFR. Thus, we cannot rule out the importance of quantifying the techniques used (eg, pressure, duration, frequency) and investigating the effects of various parameters of strain, because it may help to refine and optimize the practice of manual therapy.

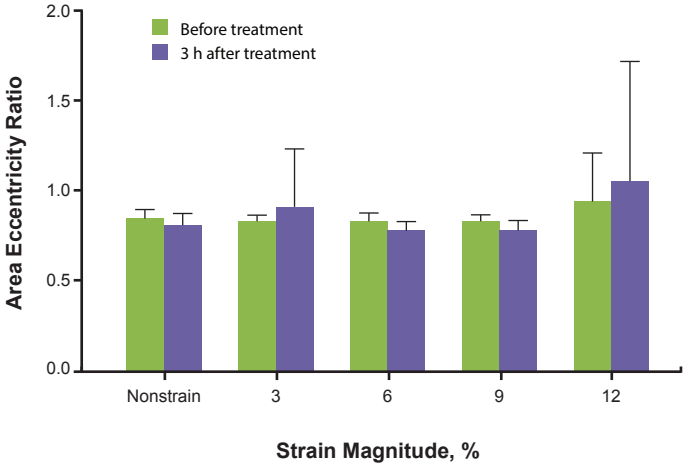

Figure 6.
Area eccentricity ratio (actual wound area ÷ by the theoretical area of an ellipse as determined by the major and minor axes [area = ½(major axis) ½(minor axis) π]) of strain magnitude comparing the area shape change before (green bars) and 3 hours after (purple bars) myofascial release. Data are presented as mean (SD).

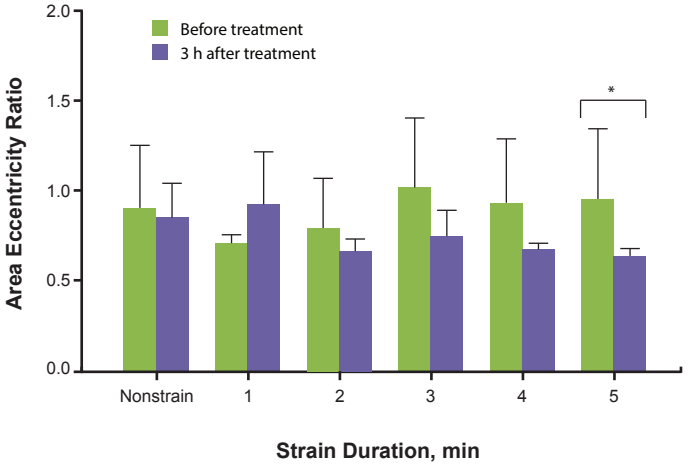

Figure 7.
Area eccentricity ratio (actual wound area ÷ by the theoretical area of an ellipse as determined by the major and minor axes [area = ½(major axis) ½(minor axis) π]) of duration of strain comparing the area shape change before (green bars) and 3 hours after (purple bars) myofascial release. Data are presented as mean (SD). The asterisk indicates $P<.05$ between pretreatment and posttreatment in the 5-minute strain group as determined by a *t* test.

Author Contributions

Mr Cao and Drs Hicks and Standley provided substantial contributions to conception and design, acquisition of data, or analysis and interpretation of data; all authors drafted the article or revised it critically for important intellectual content; and all authors gave final approval of the version of the article to be published.

References

1. Threlkeld AJ. The effects of manual therapy on connective tissue. *Phys Ther.* 1992;72(12):893-902.
2. Sucher BM. Myofascial manipulative release of carpal tunnel syndrome: documentation with magnetic resonance imaging. *J Am Osteopath Assoc.* 1993;93(12):1273-1278.
3. Hanten WP, Chandler SD. Effects of myofascial release leg pull and sagittal plane isometric contract-relax techniques on passive straight-leg raise angle. *J Orthop Sports Phys Ther.* 1994;20(3):138-144.
4. Akbari A, Moodi H, Ghiasi F, Sagheb HM, Rashidi H. Effects of vacuum-compression therapy on healing of diabetic foot ulcers: randomized controlled trial. *J Rehabil Res Dev.* 2007;44(5):631-636.
5. Blume PA, Walters J, Payne W, Ayala J, Lantis J. Comparison of negative pressure wound therapy using vacuum-assisted closure with advanced moist wound therapy in the treatment of diabetic foot ulcers: a multicenter randomized controlled trial. *Diabetes Care.* 2008;31(4):631-636.
6. McCulloch JM Jr, Kemper CC. Vacuum-compression therapy for the treatment of an ischemic ulcer. *Phys Ther.* 1993;73(3):165-169.
7. Scherer SS, Pietramaggiori G, Mathews JC, et al. The mechanism of action of the vacuum-assisted closure device. *Plast Reconstr Surg.* 2008;122(3):786-797.
8. Buckley CD, Pilling D, Lord JM, et al. Fibroblasts regulate the switch from acute resolving to chronic persistent inflammation. *Trends Immunol.* 2001;22(4):199-204.
9. Hicks MR, Cao TV, Campbell DH, Standley PR. Mechanical strain applied to human fibroblasts differentially regulates skeletal myoblast differentiation. *J Appl Physiol.* 2012;113(3):465-472.
10. McAnulty RJ. Fibroblasts and myofibroblasts: their source, function and role in disease. *Int J Biochem Cell Biol.* 2007;39(4):666-671.
11. Eagan TS, Meltzer KR, Standley PR. Importance of strain direction in regulating human fibroblast proliferation and cytokine secretion: a useful in vitro model for soft tissue injury and manual medicine treatments. *J Manipulative Physiol Ther.* 2007;30(8):584-592.
12. Meltzer KR, Cao TV, Schad JF, et al. In vitro modeling of repetitive motion injury and myofascial release. *J Bodyw Mov Ther.* 2010;14(2):162-171.
13. Meltzer KR, Standley PR. Modeled repetitive motion strain and indirect osteopathic manipulative techniques in regulation of human fibroblast proliferation and interleukin secretion. *J Am Osteopath Assoc.* 2007;107(12):527-536.
14. Cao TV, Hicks MR, Standley PR. In vitro biomechanical strain regulation of fibroblast wound healing. *J Am Osteopath Assoc.* 2013;113(11):806-818.
15. Grinnell F. Fibroblast biology in three-dimensional collagen matrices. *Trends Cell Biol.* 2003;13(5):264-269.
16. Chiu TW, Wright A. To compare the effects of different rates of application of a cervical mobilisation technique on sympathetic outflow to the upper limb in normal subjects. *Man Ther.* 1996;1(4):198-203.
17. Cao TV, Hicks MR, Campbell D, Standley PR. Dosed myofascial release in three-dimensional bioengineered tendons: effects on human fibroblast hyperplasia, hypertrophy, and cytokine secretion. *J Manipulative Physiol Ther.* 2013;36(8):513-521.
18. Mio T, Adachi Y, Romberger DJ, Ertl RF, Rennard SI. Regulation of fibroblast proliferation in three-dimensional collagen gel matrix. *In Vitro Cell Dev Biol Anim.* 1996;32(7):427-433.
19. Green JA, Yamada KM. Three-dimensional microenvironments modulate fibroblast signaling responses. *Adv Drug Deliv Rev.* 2007;59(13):1293-1298.
20. Paszek MJ, Zahir N, Johnson KR, et al. Tensional homeostasis and the malignant phenotype. *Cancer Cell.* 2005;8(3):241-254.
21. Ali S, Fritchley SJ, Chaffey BT, Kirby JA. Contribution of the putative heparan sulfate-binding motif BBXB of RANTES to transendothelial migration. *Glycobiology.* 2002;12(9):535-543.
22. Schonherr E, Hausser HJ. Extracellular matrix and cytokines: a functional unit. *Dev Immunol.* 2000;7(2-4):89-101.
23. Bush JA, Ferguson MW, Mason T, McGrouther DA. Skin tension or skin compression? small circular wounds are likely to shrink, not gape. *J Plast Reconstr Aesthet Surg.* 2008;61(5):529-534.
24. Langer K. On the anatomy and physiology of the skin I: the cleavability of the cutis. *Br J Plast Surg.* 1978;31:3-8.
25. Langer K. On the anatomy and physiology of the skin II: skin tension. *Br J Plast Surg.* 1978;31:93-106.
26. Smith RK, Birch H, Patterson-Kane J, et al. Should equine athletes commence training during skeletal development? changes in tendon matrix associated with development, ageing, function and exercise. *Equine Vet J Suppl.* 1999(30):201-209.
27. Rigozzi S, Stemmer A, Muller R, Snedeker JG. Mechanical response of individual collagen fibrils in loaded tendon as measured by atomic force microscopy. *J Struct Biol.* 2011;176(1):9-15.
28. Lee TL, Lin YC, Mochitate K, Grinnell F. Stress-relaxation of fibroblasts in collagen matrices triggers ectocytosis of plasma membrane vesicles containing actin, annexins II and VI, and beta 1 integrin receptors. *J Cell Sci.* 1993;105(pt 1):167-177.
29. Wang N, Ingber DE. Control of cytoskeletal mechanics by extracellular matrix, cell shape, and mechanical tension. *Biophys J.* 1994;66(6):2181-2189.

eTable 1.
Width Measurements of Bioengineered Tendons 48 h After Wounding by Myofascial Release Strain Duration and Magnitude (see *Figure 3*)[a]

Strain	Left	Center	Right
Magnitude (%) With 90-s Duration			
Nonstrain	1.11 (0.031)	1.08 (0.035)	1.10 (0.027)
3	1.12 (0.031)	1.09 (0.040)	1.12 (0.029)
6	1.09 (0.032)	1.08 (0.030)	1.12 (0.024)
9	1.06 (0.027)	0.96 (0.024)[b]	1.04 (0.025)
12	1.07 (0.035)	0.95 (0.048)[c]	1.05 (0.034)
Duration (s) With 6% Magnitude			
Nonstrain	1.38 (0.051)	1.39 (0.051)	1.41 (0.036)
1	1.42 (0.065)	1.40 (0.055)	1.41 (0.043)
2	1.44 (0.057)	1.41 (0.054)	1.40 (0.045)
3	1.43 (0.040)	1.40 (0.038)	1.43 (0.045)
4	1.40 (0.065)	1.35 (0.058)	1.35 (0.050)
5	144 (0 .041)	1.41 (0.044)	1.41 (0.042)

[a] Data are given as mean (SD) millimeters.
[b] Statistically significant differences ($P \leq .01$) compared with nonstrain, 3%, and 6% groups.
[c] Statistically significant differences ($P \leq .05$) compared with nonstrain, 3%, and 6% groups.

eTable 2.
Percent Change in Wound Area of Bioengineered Tendons 48 h After Wounding by Myofascial Release Strain Duration and Magnitude[a] (see *Figure 4*)

	Percent Change in Wound Area			
Magnitude, %	**3 h**	**18 h**	**24 h**	**48 h**
Nonstrain	109.12 (16.11)	85.89 (20.81)	82.16 (16.38)	66.02 (28.83)[b]
3	77.74 (25.68)	61.44 (25.10)	56.54 (23.60)[c]	49.46 (21.91)[d]
6	87.45 (17.12)	71.07 (19.46)	63.35 (19.50)	52.29 (18.49)[c]
9	95.62 (20.58)	81.52 (12.58)	75.87 (10.64)	64.96 (11.16)[e]
12	129.15 (46.89)	120.40 (42.66)	121.47 (37.80)[f]	108.19 (37.62)[g]

[a] Data are given as mean (SD). *P* values were determined using 1-way analysis of variance with post hoc Dunnett multiple comparison test.
[b] Statistically significant decrease compared with the pretreatment wound axes at time 0 ($P<.05$).
[c] Statistically significant decrease compared with the pretreatment wound axes at time 0 ($P=.01$).
[d] Statistically significant decrease compared with the pretreatment wound axes at time 0 ($P=.003$).
[e] Statistically significant decrease compared with the pretreatment wound axes at time 0 ($P=.002$).
[f] Statistically significant increase compared with the pretreatment wound axes at time 0 ($P=.01$). $P<.05$ vs nonstrain control at the same time point.
[g] Statistically significant increase compared with the pretreatment wound axes at time 0 ($P=.03$). $P<.05$ vs nonstrain control at the same time point.

eTable 3.
Percent Change in Wound Area of Bioengineered Tendons Receiving Varying Durations of Myofascial Release Strained 6% Beyond Initial Resting Length[a] (see *Figure 5*)

	Percent Change in Wound Area			
Time, min	**3 h**	**18 h**	**24 h**	**48 h**
Nonstrain	99.64 (19.98)	78.24 (20.02)	75.29 (16.80)	57.50 (26.52)[b]
1	78.46 (16.09)	62.40 (17.87)	54.35 (19.32)	48.10 (24.79)[b]
2	78.26 (27.84)	64.88 (11.16)	54.06 (22.93)[b]	43.28 (19.12)[b]
3	68.50 (18.30)[c]	57.88 (20.15)[b]	52.50 (22.21)[b]	45.24 (24.81)[b]
4	74.43 (9.11)	61.73 (11.47)[c]	61.58 (6.48)	32.78 (19.08)[b]
5	59.91(17.77)[c]	50.24 (19.01)[b]	43.12 (17.24)[b]	26.97 (14.47)[b]

[a] Data are given as mean (SD). Changes in wound area measured as a percent change from time 0 (100%) measured 3, 18, 24, and 48 h after myofascial release. *P* values were determined using 1-way analysis of variance with post hoc Dunnett multiple comparison test.
[b] Statistically significant decrease ($P\leq.03$) in wound area compared with time 0.
[c] Statistically significant decrease ($P<.05$) in wound area compare with time 0.